Ortho-para separation of molecules using optical orientation of atoms in hyperfine Zeeman states

Chun He
Molecular Physics Laboratory, SRI International, Menlo Park, California 94025
(Received 13 February 1997; revised manuscript received 5 September 1997)

Ortho-para separations of $^7Li_2$ and $^6Li_2$ molecules were achieved by using a monochromatic laser beam to align atoms into a single nuclear spin state. This approach is unlike the cryogenic cooling technique, which has been successful only on very light molecules (such as H_2 and D_2), which have large energy gaps between the lowest rotational states. The atoms were ''pumped into'' a single hyperfine Zeeman state with defined electron and nuclear spin orientations. The well-resolved rotational structures of the lithium molecules, as shown by laser-induced fluorescence spectra, revealed the enrichment of ortho-components over para-components. Using laser radiation with a power density of ~ 10 mW/cm^2 can increase the amount of ortho-components by a factor of 2 for $^7Li_2$ vapor and by a factor of 3 for $^6Li_2$ vapor on a time scale of milliseconds. This paper proposes a model to account for the experimental observations. These increases in the concentrations of ortho-components to para-components are explained by a combined effect of (i) a decrease in molecular density due to the electron spin orientation and (ii) a transfer of nuclear spin momenta from oriented atoms to molecules. The exchange reaction, $Li' + Li_2 \rightarrow Li_3 \rightarrow Li' Li + Li$, appears to transfer the spin orientation from atoms to molecules. A substantial number of ortho-para separations can be achieved through multiple exchange collisions. Applications of this technique to other homonuclear diatomic molecules and polyatomic molecules with nuclear exchange symmetry are predicted. [S1050-2947(98)02205-7]

PACS number(s): 33.25.+k, 33.15.Pw, 33.20.Bx

I. INTRODUCTION

The ortho and para forms of homonuclear diatomic molecules and molecules with a nuclear exchange symmetry are intrinsic properties originating from wave functions of their nuclear spin states. The requirement that the overall molecular wave function be symmetric or antisymmetric with respect to the exchange of two or more identical nuclei restricts the rovibrational states that each form can have [1]. The ortho- and para-molecules each occupy rovibrational energy levels that differ from each other by one rotational quantum number. Generally, the two forms mix together and reach an equilibrium composition determined by the number of nuclear spin wave functions each form has. At extremely low temperatures, the occupation of each form is also influenced by the thermal statistical weight that influences the population of the lowest rovibrational energy levels.

Ortho-para separation, or the shift of molecules from their thermal equilibrium values, has long been sought because of important applications in fundamental studies (such as nuclear spin relaxation and ortho-para transition) and in practical applications (such as recent work on the magnetic resonance image of lungs) [2]. However, separation of any molecule other than H_2 or D_2 in which the ratio of the concentrations of the different nuclear spin symmetry species is different from the high-temperature equilibrium value has not been reported [3].

The separation of H_2 or D_2 was achieved over several months by cryogenic cooling, taking advantage of the large energy separation between the lowest states of the two forms [4]. For example, the lowest state of para-H_2 is separated from the lowest state of ortho-H_2 by a rotational energy equivalent of 175 K (122 cm^{-1}), allowing enrichment of para-H_2 at low temperature; the para-H_2 can then be warmed up without a change of nuclear spin state.

Obviously, this method cannot be applied to the rest of the homonuclear diatomic molecules, because of the smaller rotational energy spacing between the two forms resulting from increased molecular weights. For example, the energy separation between the lowest state of para-$^7Li_2$ and the lowest state of ortho-$^7Li_2$ has a temperature equivalent of less than 2 K, and this separation is merely 0.1 K in $^{127}I_2$, a temperature well below the freezing point of these elements. Many alternative methods have been suggested and attempted without success [4,5].

Here, I report a method for obtaining a very large degree of ortho and para separation of homonuclear diatomic molecules. The effectiveness of this method was demonstrated in experiments performed on isotopically pure $^7Li_2$ and $^6Li_2$ molecules, in which the concentrations of ortho-$^7Li_2$ and ortho-$^6Li_2$ were increased by a factor of 2 and 3, respectively [6–8]. I achieved separation in two steps: (i) by establishing a nuclear spin orientation in atoms and (ii) by transferring the nuclear spin orientation to molecules through atom exchange collisions. The orientation of nuclear spin in the atoms was achieved by optical pumping within hyperfine Zeeman states. I have achieved over 50% efficiency of such atomic orientation into a single nuclear spin state for both ^{7}Li and ^{6}Li atomic vapors [6]. Happer [9] reported that a 100% spin orientation in Na atoms was achieved using a sophisticated cell coating technique to minimize spin relaxation from collisions with cell walls.

II. EXPERIMENTAL PROCEDURES

The experimental arrangement was described previously [6,7]. The diatomic molecules were generated in a stainless-steel pipe cross charged with isotopically pure ^{7}Li or ^{6}Li and He buffer gas. The buffer gas protects the nuclear spin oriented atom from diffusing to the walls of the vapor cell

(where the spin orientation can be destroyed at high efficiency) before colliding with a molecule. The experiments were performed between 550 and 650 K for both ^{7}Li and ^{6}Li, with buffer pressures of 200 torr for ^{7}Li and 50 torr for ^{6}Li. Vapor pressures of Li and Li_2 were 1.98×10^{-7} to 3.66×10^{-5} torr and 9.7×10^{-11} to 1.98×10^{-8} torr, respectively, at the above heating temperatures [10]. A steady magnetic field of 40 G was applied to the cell with a pair of 12-in.-diam Helmholtz coils. This field was of sufficient magnitude to overcome disorientation effects due to stray, time-dependent magnetic fields, and it produced a splitting of 28 MHz between hyperfine Zeeman states of the ground state $2\,^2S_{1/2}$ and a splitting of 9.34 MHz between the hyperfine Zeeman states of the $2\,^2P_{1/2}$ excited state [6,11].

Without the steady applied magnetic field, nuclear spin orientation could not be produced. The nuclear spin polarization of ^{7}Li or ^{6}Li atoms is produced with a circularly polarized, single mode cw dye laser tuned to the D_1 resonance transition ($2\,^2P_{1/2}\leftarrow 2\,^2S_{1/2}$) at 670.79 nm, propagating through the cell parallel to the magnetic field [6,11]. The laser linewidth was not determined, but was estimated to be $\sim$10 MHz according to the manufacturer. With a beam diameter of 5 mm and a typical output power of 10 mW, the laser power density used in the experiment is about 50 mW/cm^2. In the ground state, orientation consists of a preferred population of one of the magnetic sublevels with either maximum M_F (if the direction of circular polarization is along the direction of the magnetic field) or minimum M_F (if the direction of circular polarization is counter to the direction of the magnetic field) [6]. The preferred population at a single M_F level is due to the transition selection rule of $\Delta M_F=+1$, under the excitation of a σ^+-polarized photon, or $\Delta M_F=-1$, under the excitation of a σ^--polarized photon.

Atoms in all the hyperfine Zeeman levels belonging to the $2\,^2S_{1/2}$ state can be excited to the $2\,^2P_{1/2}$ excited state *except* for atoms in the maximum M_F level ($F=2, M_F=2$) for σ^+-polarized photon excitation or atoms in the minimum M_F level ($F=2, M_F=-2$) for σ^--polarized photon excitation. Atoms in the $2\,^2P_{1/2}$ excited state can, however, spontaneously radiate to *all* levels of the $2\,^2S_{1/2}$ ground state and be reexcited by the laser, ultimately producing atomic orientation in the single hyperfine Zeeman level, ($F=2, M_F=2$) or ($F=2, M_F=-2$). The hyperfine Zeeman transitions can be pumped at a single laser wavelength because the spacing (37.33 MHz) between the spectral lines of the allowed hyperfine Zeeman states transitions under the D_1 profile is much smaller than the line broadening (a few GHz) at cell pressures of 50–200 torr [12].

The laser frequency is carefully tuned to avoid inducing atomic transitions to the $2\,^2P_{3/2}$ manifold, which is located 9.28 GHz above the $2\,^2P_{1/2}$ manifold. Atomic orientation cannot be achieved with a D_2 transition ($2\,^2P_{3/2}\leftarrow 2\,^2S_{1/2}$), because *all* hyperfine Zeeman levels in the $2\,^2S_{1/2}$ ground state allow transitions to the $2\,^2P_{3/2}$ manifold. Figure 1 shows the energy level diagram and the relevant transitions of a ^{7}Li atom influenced by a σ^+-polarized photon tuned to the D_1 transition.

The ortho and para composition and rotational state distributions of Li_2 are monitored by using the laser-induced fluorescence (LIF) method, with a second tunable cw dye laser of 1 cm^{-1} bandwidth propagating counter to the atomic pumping laser in the vapor cell. Molecular fluorescence from the $A\,^1\Sigma_u^+\leftarrow X\,^1\Sigma_g^+$ transition is detected by a phase-sensitive detector consisting of a monochromator-filter combination, a photomultiplier, and a lock-in amplifier.

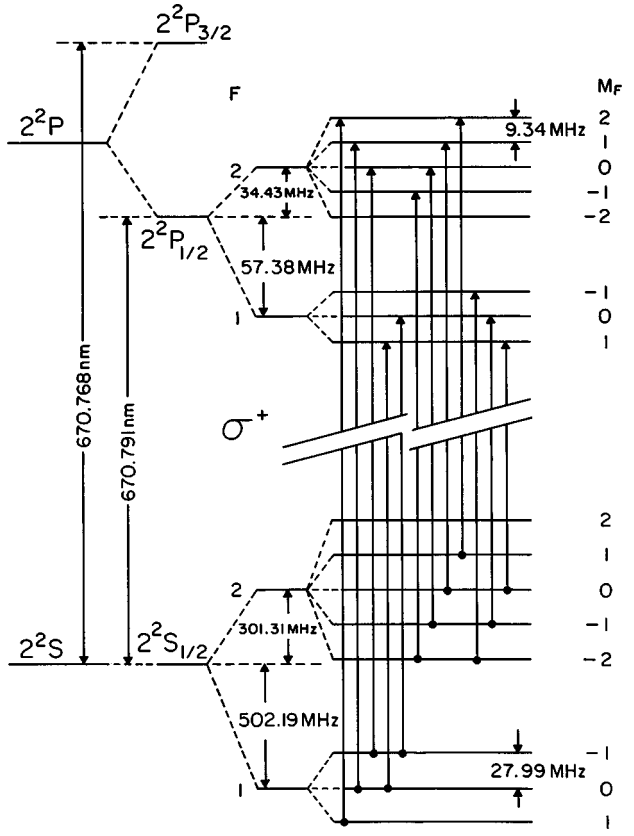

FIG. 1. The energy level diagram of ^{7}Li including the spin-orbital interaction (fine structure), the interaction of the electron with the atomic nucleus (hyperfine structure), and the Zeeman effect. The arrows indicate the allowed transitions $\Delta m_F=+1$ under a σ^+-polarized excitation. The Zeeman splittings are calculated for an external field of 40 G. The graph is not drawn to scale.

III. RESULTS AND DISCUSSION

A small segment of the excitation spectrum of $^7Li_2$ is recorded when either the static, applied magnetic field or the optical pumping laser or both are tuned off. This condition represents the absence of atomic orientation in the cell. When the power of the optical pumping laser is not zero and the applied field is tuned to 40 G, with its direction parallel to the optical pumping radiation, the same segment of the $^7Li_2$ spectrum is scanned again. Figure 2 shows the results for a segment composed mainly of $A\,^1\Sigma_u^+(v=2)\leftarrow X\,^1\Sigma_g^+(v=0)$ transitions at an optical pumping laser power density of 36 mW/cm^2. Some lines are blends of several transitions, but other lines give a clearly resolved measure of the concentrations of ortho-$^7Li_2$ and para-$^7Li_2$, which accompany the atomic nuclear spin orientation.

Several features are immediately evident. Transitions that originate from even J rotational levels in the ground $X\,^1\Sigma_g^+$ state decrease in intensity upon production of the ^{7}Li atomic nuclear orientation. These are para-$^7Li_2$ species having a to-

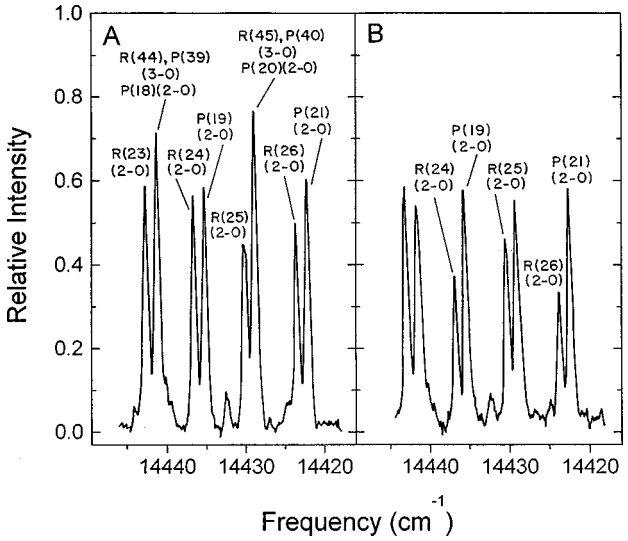

FIG. 2. A segment of the $^7Li_2$, $A\,^1\Sigma_u^+ \leftarrow X\,^1\Sigma_g^+$ laser-induced fluorescence spectrum (A) in the absence of the $^7Li_2$ atomic spin orientation and (B) in the presence of the $^7Li_2$ atomic spin orientation at a laser power density of 30 mW/cm^2, showing the change in several $X\,^1\Sigma_g^+$ ($v=0$) rotational level populations.

tal nuclear spin of $T=2$ or 0, because the ^{7}Li nuclear spin is $I=3/2$. Transitions that originate from ground state levels with odd values of J retain nearly the same intensity in the presence of the ^{7}Li nuclear orientation in the example shown in Fig. 2. These are ortho-$^7Li_2$ molecules having a total nuclear spin of $T=3$ or 1. The two spectral lines that are blends of transitions from ortho-$^7Li_2$ and para-$^7Li_2$ decrease in intensity, because they are composed mainly of transitions from para-$^7Li_2$ [$P(18)(2\text{-}0)$ and $P(20)(2\text{-}0)$]. The overall change in concentration of ortho-$^7Li_2$ and para-$^7Li_2$ can be found by averaging the intensities of the completely resolved transitions from the $X\,^1\Sigma_g^+$ state of ortho-$^7Li_2$ and para-$^7Li_2$, weighted by the proper line strength functions and the Boltzmann factor, although these corrections are negligible.

Table I shows the effects of increasing power density of the optical pumping laser on several $A\,^1\Sigma_u^+(v=2) \leftarrow X\,^1\Sigma_g^+(v=0)$ $^7Li_2$ spectral line intensities, normalized to zero laser power, the ortho-$^7Li_2$ and para-$^7Li_2$ concentration ratio, and the degree of spin orientation Θ. The degree of spin orientation, as defined in the Appendix, is determined by atomic fluorescence intensities measured in the presence and absence of the magnetic field. Here the normalized intensity of a spectral line is

$$\frac{N}{N^0} \equiv \frac{F_M(P)}{F_M(P=0)}$$

and the ortho-para concentration ratio is

$$K(\text{ortho-para ratio}) \equiv \frac{[\text{ortho-}Li_2]}{[\text{para-}Li_2]},$$

where $F_M(P=0)$ is the molecular fluorescence intensity measured when there is no atomic orientation, $F_M(P)$ is the molecular fluorescence intensity measured at the value of the laser power given by P, and [ortho-$^7Li_2$] and [para-$^7Li_2$] are the concentrations of ortho-$^7Li_2$ and ortho-$^7Li_2$, respectively.

The relative concentration of ortho-$^7Li_2$ to para-$^7Li_2$ increases with the laser power, reaching a value of 5.17 at a power density of 75.4 mW/cm^2, which represents an enrichment factor of 3 in the concentration of ortho-$^7Li_2$ compared with its natural abundance. Figure 3 shows how the normalized intensities of the well-resolved $^7Li_2$ spectral lines depend on the power of the optical pumping laser.

Equivalent experiments were performed on isotopically pure $^6Li_2$ molecules. Trace A in Fig. 4 shows a small segment of the LIF spectrum of the $A\,^1\Sigma_u^+ \leftarrow X\,^1\Sigma_g^+$ transition of $^6Li_2$ when there is no atomic orientation in the vapor cell. When the atomic orientation is produced in the cell, by radiating the $A\,^1\Sigma_u^+ \leftarrow X\,^1\Sigma_g^+$ transition of $^6Li_2$ with 2.5 mW/cm^2 of laser power density, the LIF of the same segment of the $^6Li_2$ spectrum is scanned again to give the results shown by trace B. These spectra consist primarily of $A\,^1\Sigma_u^+(v=1) \leftarrow X\,^1\Sigma_g^+(v=0)$ transitions. Again, some spectral lines are blends of several transitions, but many transitions are clearly resolved and show the changes in popula-

TABLE I. Effects of optical pumping laser power on changes in normalized intensities of several observed $A^1\Sigma_u^+(v=2) \leftarrow X^1\Sigma_g^+(v=0)$ $^7Li_2$ spectral line intensities, N/N^0, degree of spin orientation of atom ^{7}Li, Θ, and composition change on ortho-$^7Li_2$ and para-$^7Li_2$ concentrations, K(ortho-para ratio).

		Change in relative intensity (N/N^0)						
Optical pumping laser power		Para			Ortho			
(10^{-3} W/cm^2)	Θ	$R(26)$	$R(24)$	$P(21)$	$R(25)$	$P(19)$	$R(23)$	K(ortho-para ratio)
0.0	0.0	1.0	1.0	1.0	1.0	1.0	1.0	5/3=1.67
0.71	0.03	0.90	0.86	1.00	0.97	1.02	1.01	3.19
1.83	0.04	0.75	0.76	1.02	1.00	1.06	1.03	3.81
3.87	0.06	0.59	0.63	0.97	0.94	0.97	1.01	4.44
8.96	0.10	0.57	0.58	0.94	0.96	0.96	0.92	4.58
17.3	0.16	0.56	0.56	0.95	0.99	0.97	0.94	4.79
35.7	0.22	0.55	0.55	0.93	0.93	0.94	0.94	4.72
75.4	0.26	0.51	0.52	0.98	0.99	0.98	0.92	5.17

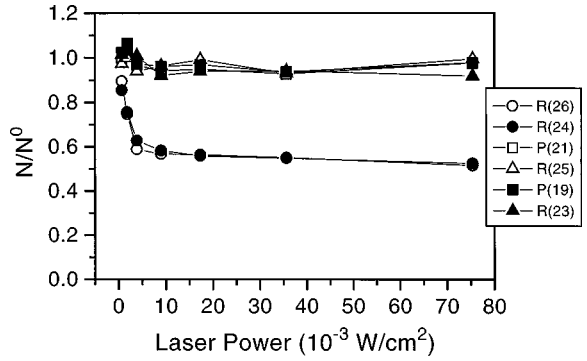

FIG. 3. Normalized intensities N/N^0 for several completely resolved rotational lines in the $A\,^1\Sigma_u^+(v=2)\leftarrow X\,^1\Sigma_g^+(v=0)$ transition for $^7Li_2$ as a function of laser power.

tion of several $X\,^1\Sigma_g^+$ rotational levels that accompany the atomic orientation produced by an optical pumping laser.

Transitions that originate from odd J rotational levels in the ground $X\,^1\Sigma_g^+$ state decrease in intensity on production of the ^{6}Li atomic orientation. These are the para-$^6Li_2$ species having a total nuclear spin of $T=1$, because the ^{6}Li nuclear spin is $I=1$. Transitions that originate from ground state levels with even values of J retain nearly the same intensity in the presence of the Li atomic orientation as the example shown in Fig. 4. These are the para-$^6Li_2$ species having a total nuclear spin of $T=2$ or 0. The spectral lines that are blends of transitions from both ortho and para states decrease in intensity. Table II shows the effects of increasing power density of the optical pumping laser on the relative intensities of observed $A\,^1\Sigma_u^+(v=1)\leftarrow X\,^1\Sigma_g^+(v=0)$ $^6Li_2$ spectral lines N/N^0 and composition changes in ortho-$^6Li_2$ and para-$^6Li_2$ concentrations K, as well as the degree of spin orientation Θ upon optical pumping. Figure 5 shows the effects of optical pumping on the relative intensities of the observed $^6Li_2$ lines.

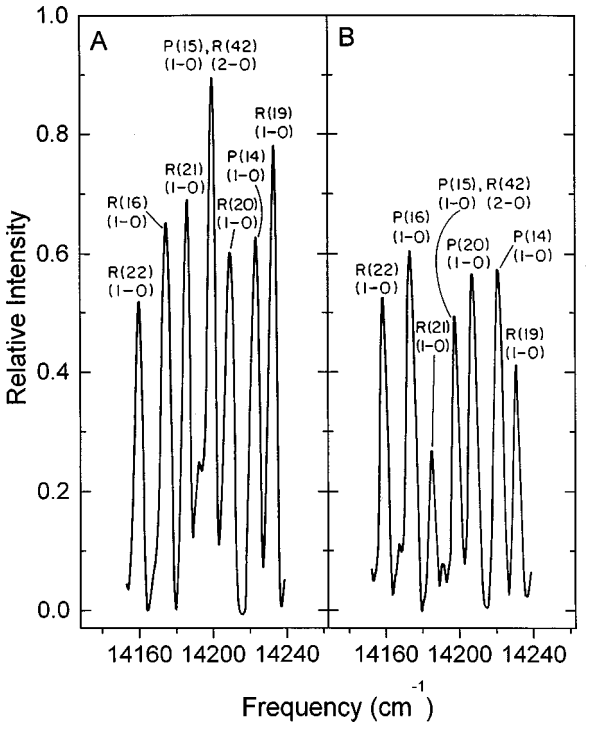

FIG. 4. A segment of the $^6Li_2$, $A\,^1\Sigma_u^+\leftarrow X\,^1\Sigma_g^+$ laser-induced fluorescence spectrum (A) in the absence of the ^{6}Li atomic spin orientation and (B) in the presence of the ^{6}Li atomic spin orientation at a laser power density of 2.5 mW/cm^2, showing the change in several $X\,^1\Sigma_g^+(v=0)$ rotational level populations.

The experimental results for ^{7}Li and ^{6}Li are very similar. In both cases, the para molecules exhibit a large shift in population with atomic orientation. In ^{7}Li, the para species have even-numbered J values, whereas in ^{6}Li, the para species have odd-numbered J values. These changes in the ortho-para ratio represent a net composition change in the diatomic molecules in the vapor cell, with ortho species being favored.

IV. MECHANISM

I propose a simple mechanism to explain the ortho-para separation induced by the nuclear spin orientation of atoms. The vapor composition in the lithium heat pipe is determined by the following three processes: (i) formation of a lithium dimer by atomic collisions,

$$\mathrm{Li}+\mathrm{Li}+M\xrightarrow{k_1}\mathrm{Li}_2+M; \tag{1}$$

(ii) dissociation of Li_2,

$$\mathrm{Li}_2+M\xrightarrow{k_2}2\mathrm{Li}+M; \tag{2}$$

(iii) atom exchange,

$$\mathrm{Li}_2+\mathrm{Li}'\xrightarrow{k_3}\mathrm{LiLi}'+\mathrm{Li}, \tag{3}$$

where M is a third body that can be an atom of lithium or helium buffer gas. The concentrations of lithium atoms and molecules in the heat pipe are determined by the rate of atomic association (k_1) and the rate of molecular dissociation (k_2). The exchange reaction does not influence the overall concentrations of atoms and molecules; however, it is the only pathway that accounts for the ortho-para separation observed in the experiments. The experiment results, induced by an atomic electron and nuclear spin orientation, can be explained as the combined effect of (i) a decrease in molecular density and (ii) a shift in nuclear spin distribution.

A. Decrease in molecular density

The association of atoms to form dimers described by Eq. (1) depends not only on the concentration of atoms but also on the spin states of the unpaired electrons. Based on their relative spin orientation, the combination of two atoms gives rise to two potential curves having total spin singlet and triplet multiplicities, with the singlet being bonding and the triplet antibonding. If the electron spins of the colliding pair are antiparallel ($S=0$), the collision will proceed along the singlet bonding channel and a molecular formation can occur, with a third body M carrying away energy. If the two electrons spins are parallel ($S=1$), the collision trajectory follows a triplet antibonding curve and no molecular formation occurs. In fact, because two single-electron atoms can

TABLE II. Effects of optical pumping laser power on changes in normalized intensities of several observed $A\ ^1\Sigma_u^+(v=1)\leftarrow X\ ^1\Sigma_g^+(v=0)$ $^6Li_2$ spectral line intensities, N/N^0, degree of spin orientation of atom ^{6}Li, Θ, and composition change on ortho-$^6Li_2$ and para-$^6Li_2$ concentrations, K(ortho-para ratio).

		Change in relative intensity (N/N^0)						
Optical pumping laser power (10^{-3} W/cm^2)		Para		Ortho				
	Θ	$R(19)$	$R(21)$	$P(14)$	$R(20)$	$P(16)$	$R(22)$	K(ortho-para ratio)
0.0	0.0	1.0	1.0	1.0	1.0	1.0	1.0	2.0
0.255	0.005	0.900	0.880	0.995	0.996	0.995	0.993	2.24
0.509	0.01	0.732	0.709	0.965	0.937	0.924	0.986	2.65
1.019	0.02	0.578	0.609	0.932	0.911	0.860	0.860	3.00
1.81	0.10	0.525	0.520	0.838	0.930	0.897	0.867	3.38
2.55	0.16	0.487	0.430	0.896	0.859	0.840	0.870	3.78
4.28	0.20	0.450	0.440	0.961	1.016	1.018	0.884	4.36
5.45	0.23	0.420	0.390	0.954	0.987	0.921	0.824	4.55
7.13	0.27	0.390	0.410	0.916	1.031	0.930	0.898	4.72
10.19	0.26	0.435	0.370	0.937	1.006	1.036	0.978	4.92
15.28	0.31	0.390	0.395	0.882	1.007	1.046	0.901	4.89
25.46	0.33	0.380	0.450	0.885	1.006	0.964	0.923	4.55
40.74	0.34	0.438	0.387	0.959	0.916	0.947	0.983	4.61
53.99	0.34	0.398	0.392	0.908	1.000	1.088	0.913	4.95
66.21	0.35	0.420	0.380	1.067	1.045	1.000	1.100	5.27
86.58	0.35	0.370	0.293	1.065	1.089	0.999	1.135	6.48

form three symmetric and one antisymmetric wave function, only 25% of the Li-Li collisions have the proper spin requirements ($S=0$) for molecular formation.

I limit this discussion to the experiment on ^{7}Li vapor and assume that a σ^+-polarized laser is being used. However, the discussion and conclusions are also valid for experiments on ^{6}Li vapor and for a σ^--polarized laser.

The optical pumping produces ^{7}Li atoms in the specific quantum state $\{F=2, M_F=2, 2\ ^2S_{1/2}\}$. This means that both the electron spin and the nuclear spin have been spin oriented with $\{s=1/2, m_s=1/2\}$ for the electrons and $\{I=3/2, m_I=3/2\}$ for the nuclei. The bonding and antibonding trajectories of two atoms are determined by the quantum states of their electron spins rather than by their nuclear spins, because the energy resulting from the coupling of nuclear spins is too weak to influence the bonding characters of the two atoms.

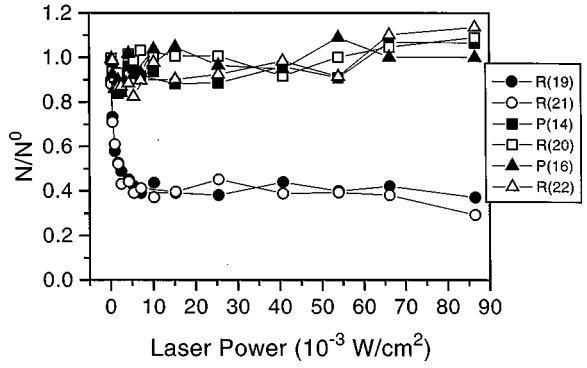

FIG. 5. Normalized intensities N/N^0 for several completely resolved rotational lines in the $A\ ^1\Sigma_u^+(v=1)\leftarrow X\ ^1\Sigma_g^+(v=0)$ transition for $^6Li_2$ as a function of laser power.

It is easy to show that, among the hyperfine states M_F ($M_F=2,1,0,-1,-2$), the occurrence of hyperfine Zeeman states having electron spin projection $m_s=1/2$ is the same as that for having electron spin projection $m_s=-1/2$. Without optical orientation, the atoms in the vapor are near-evenly populated in these hyperfine Zeeman levels designated by M_F, and there are as many atoms with $m_s=1/2$ as with $m_s=-1/2$ in the vapor. The possibility of a collision between an atom with $m_s=1/2$ and one with $m_s=-1/2$ is at a maximum. With σ^+-polarized optical pumping, the $\{F=2, M_F=2\}$ level is more densely populated than the other levels. The total number of atomic collisions with antiparallel electron spins is then reduced, because the number of atoms with electron spin quantum number $m_s=1/2$ is greater than those with $m_s=-1/2$. As a consequence, the total number of molecules in the vapor will decrease.

B. Shift in ortho and para distribution

Without atomic spin orientation, the ^{7}Li atoms are evenly distributed among the hyperfine Zeeman levels of the ground state as shown in Fig. 6 (A). Exchange collisions between atoms and molecules do not influence the ortho- or para-status of the molecules. The ortho-$^7Li_2$ has ten symmetric nuclear spin wave functions with a total nuclear spin quantum number $T=3$ or 1, and the para-$^7Li_2$ has six antisymmetric nuclear spin wave functions with a quantum number $T=0$ or 2. Therefore, each exchange collision will have a 5/8 probability of producing an ortho-$^7Li_2$ and a 3/8 probability of producing a para-$^7Li_2$, resulting in a 5:3 equilibrium concentration ratio of ortho-$^7Li_2$ to para-$^7Li_2$.

When atomic spin orientation is established in the vapor, ^{7}Li atoms are no longer distributed evenly among the hyperfine Zeeman levels, but are preferentially populated in the

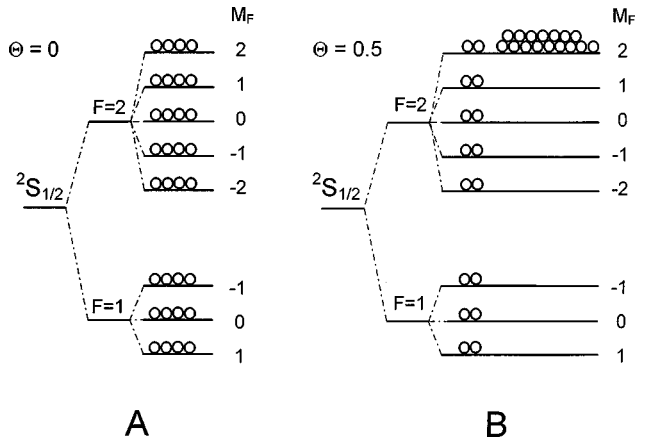

FIG. 6. Pictorial representations of atomic distribution (A) before and (B) after atomic optical pumping.

($F=2, M_F=2$) level of the $2\,^2S_{1/2}$ ground state [Fig. 6 (B)]. This distribution can be characterized by a parameter, the degree of spin orientation Θ, which is defined as (see the Appendix)

$$\Theta \equiv \frac{n_a - \langle n^{(k-1)} \rangle}{N}$$

with

$$\langle n^{(k-1)} \rangle = \frac{\sum_{i \neq a} n_i}{k-1} \quad \text{and} \quad N = \sum n_i , \tag{4}$$

where n_a is the population of atoms in the ($F=2, M_F=2$) level, n_i is population of atoms in the ith level, k is the total number of energy levels in the ground state involved in the optical pumping transitions, $\langle n^{(k-1)} \rangle$ is the average population of atoms over the $(k-1)$ hyperfine Zeeman levels from which the atoms are being pumped, and N is the total population of atoms in the ground state manifold. $\Theta=1$ represents 100% spin orientation in which all atoms are in the ($F=2, M_F=2$) level of the $2\,^2S_{1/2}$ ground state; $\Theta=0$ represents atoms randomly populated among the magnetic sublevels [13]. The Θ value depends on the optical pumping efficiency and the rate of spin relaxation.

If the nuclear spin polarization is transferred from atoms to a molecule during the exchange collisions, the resultant molecule will have a total nuclear spin quantum number $T=3$, which is an ortho-$^7Li_2$. The $T=3$ (ortho) modification of $^7Li_2$ is favored at the expense of the other molecular nuclear spin states, because the exchange reaction does not influence the total number of molecules. The net result is a conversion of para-$^7Li_2$ to ortho-$^7Li_2$. Therefore, the abundance of ortho-$^7Li_2$ is increased, accompanied by a decrease of para-$^7Li_2$. This is in agreement with our experimental results.

For ^{6}Li vapor, after optical pumping by a σ^+-polarized laser, the ^{6}Li atoms are spin oriented with a population concentrated in the $\{F=3/2, M_F=3/2, 2\,^2S_{1/2}\}$ ground state. If the atomic nuclear spin orientation is transferred to the $^6Li_2$ molecule, the resultant $^6Li_2$ molecule will have a total nuclear spin quantum number $T=2$. This is also an ortho-$^6Li_2$ but corresponds to states with *even* rotational quantum number J (in contrast to ortho-$^7Li_2$, which corresponds to *odd* J) because the nuclei of ^{6}Li are bosons while the nuclei of ^{7}Li are fermions. Similar to the situation for $^7Li_2$, the net result of optical pumping will be an increase in the intensity of transitions that originated from even J states.

Several theoretical studies discuss alkali-metal atom-molecule exchange reactions [14–16]. Whitehead [15] used a classical trajectory calculation to show that the exchange reaction $Li+Li_2 \rightarrow Li_2+Li$ proceeds via a stable intermediate, Li_3, which has a potential well of depth that is 8.30 kcal mol^{-1} lower in energy than $Li+Li_2$. The existence of such a stable intermediate for this reaction likely gives rise to a long-lived collision complex at lower collisional energies. At a collisional energy of 1 kcal mol^{-1} (equivalent to the thermal energy at 503 K, the energy closest to the 623 K of the present experiment), the collisional cross section is 115 Å. The reaction proceeds along the potential-energy surface via a nonrigid, nonlinear complex that exists for several vibrational periods of the triatomic complex. At a collisional energy of 1 kcal mol^{-1}, the average lifetime of the Li_3 complex is 3.55 ps. With a vibrational period of 0.1 ps, the complex vibrates more than 35 times before it dissociates [15].

The accuracy of this classical trajectory calculation is supported by the later *ab initio* calculation of the electronic ground state of Li_3 performed by Gerber and Schumacher [16]. From their calculation, the triangular geometry of the complex has the optimum configuration for the lowest vibrational state with a dissociation channel $Li_3 \rightarrow Li_2+Li$ that lies 3000 cm^{-1} (8.57 kcal mol^{-1}) above the zero-point vibronic level, which agrees quite well with the calculation of Whitehead (8.30 kcal mol^{-1}). These theoretical calculations are further supported by the observation of a stable lithium trimer in an excited electronic state [17].

In contrast to the fairly precise characterization of the atom-molecule exchange reaction, there is a lack of theoretical treatment of exchange reactions between oriented atoms and molecules. In the following discussion, we propose a simple mechanism to describe how the Li_2 molecule becomes oriented in the $T=3$ ($^7Li_2$) or $T=2$ ($^6Li_2$) nuclear spin state after collision with spin oriented lithium atoms.

Although the general mechanism of the elementary reaction studies involving altered electron configurations is complicated, the evolution of the nuclear (and electron) spins can readily be described in terms of the spin conservation and the weakness of the spin-spin interaction. The characteristic energy shift caused by the nuclear spin-spin interaction (fine structure in NMR spectra) is several hundred hertz, and that caused by the electron-nuclear spin interaction (hyperfine) is typically several hundred megahertz. From the uncertainty principle $\Delta E \Delta t \geqslant h/2$, one can find that the characteristic time of the nuclear spin-spin interaction is 10^{-7} s, and that of the electron-nuclear spin interaction is 10^{-10} s. Moreover, the classical trajectory calculation gives the lifetime of the Li_3 intermediate transition state to be 10^{-12} s [15]. Thus, the spin projections of all nuclei would be conserved during the exchange reaction, and a change in spin states of the Li atom and Li_2 molecule can occur solely upon the transition of a nucleus from one collision partner to another.

When the transition complex Li_3 decays, it can lose either (a) the initial Li atom, which attacked the Li_2 before the

TABLE III. Probability distribution for product formation in the $^1H+{}^1H_2\rightarrow{}^1H_2+{}^1H$ exchange reaction via a linear $^1H_3$ transition state.

	Products						
Reactants	$\alpha+\alpha\alpha$	$\alpha+(\alpha\beta+\beta\alpha)$	$\alpha+(\alpha\beta-\beta\alpha)$	$\beta+\alpha\alpha$	$\alpha+\beta\beta$	$\beta+(\alpha\beta+\beta\alpha)$	$\beta+(\alpha\beta-\beta\alpha)$
$\alpha+\alpha\alpha$	1						
$\alpha+(\alpha\beta+\beta\alpha)$		3/8	3/8	1/4			
$\alpha+(\alpha\beta-\beta\alpha)$		3/8	3/8	1/4			
$\alpha+\beta\beta$					1/2	1/4	1/4

complex formation, or (b) a different Li atom, which was originally a component of Li_2. For case (a), no changes occur in the spin states of the particles. However, in case (b), the nuclear spin orientation in the Li atom can be transferred to the molecule. Because the $^7Li_2$ has as many as 16 nuclear spin states ($^6Li_2$ has 9), quantitative calculations are tedious. The $^1H+{}^1H_2$ exchange collision provides a simplified example. The conclusion, however, can be applied to the present experimental results for $^7Li_2$ and $^6Li_2$.

The nuclear spin states $m_I=1/2$ and $m_I=-1/2$ for protons in $^1H_2$ are referred to here as α and β, respectively. If ^1H atoms are spin oriented in the α state, the following four collisions occur:

$$\alpha+\alpha\alpha,$$

$$\alpha+(\alpha\beta+\beta\alpha),$$

$$\alpha+(\alpha\beta-\beta\alpha),$$

$$\alpha+\beta\beta.$$

Different configurations of the $^1H_3$ complex will give different reaction rates of exchange collisions, because the probability of detaching each atom is different. When the complex has a linear configuration, the probability of restoring the initial state is 1/2. When the complex has a triangular configuration, the probability is reduced to 1/3. The results are shown in Tables III and IV. Summation over each column gives the probability of forming the $^1H_2$ molecule with a specific total nuclear spin state. For the triangular complex, the probability distribution for each nuclear spin state is

$$\alpha\alpha:(\alpha\beta+\beta\alpha):(\alpha\beta-\beta\alpha):\beta\beta$$
$$=5:3:3:1 \quad \text{for the 1st collision,}$$

$$\alpha\alpha:(\alpha\beta+\beta\alpha):(\alpha\beta-\beta\alpha):\beta\beta$$
$$=21:7:7:1 \quad \text{for the 2nd collision,}$$

$$\alpha\alpha:(\alpha\beta+\beta\alpha):(\alpha\beta-\beta\alpha):\beta\beta$$
$$=77:15:15:1 \quad \text{for the 3rd collision,}$$

$$\alpha\alpha:(\alpha\beta+\beta\alpha):(\alpha\beta-\beta\alpha):\beta\beta$$
$$=261:31:31:1 \quad \text{for the 4th collision.}$$

These ratios clearly show that the total nuclear spin state of $T=1$ ($\alpha\alpha$) of $^1H_2$ is favored after the multiple exchange collision. One expects corresponding conclusions for $^7Li_2$ and $^6Li_2$.

V. FINAL REMARKS

Can this experimental methodology and the theoretical model be applied to other molecules? The answer is yes. The essence of this approach on ortho-para separation is to first establish the nuclear spin orientation in atoms, and then to transfer this orientation to molecules through multiple, chemical exchange collisions, thus achieving ortho-para separation in the molecules. To accomplish this, we must establish a physical environment in which atoms and molecules coexist. At appropriate temperatures, ^7Li and ^6Li metal vapors represent such entities to us.

We can apply this methodology to other alkali-metal metals, such as isotopes of Na, K, Rb, and Cs. Weber and Stock observed the presence of nuclear spin polarization on $^{23}Na_2$ more than 20 years ago [18]. Using an approach identical to that described here, I also observed an ortho over para enrichment in $^{23}Na_2$ [19]. Ortho-para separations can be performed on other molecules. The homonuclear diatomic molecules and the symmetric top polyatomic molecules are the first categories within the immediate expansion. Among them, the simplest systems could be O_2, S_2, NH_3, halogen dimers, and CH_3X, where X is an atom or a function group.

For these molecules, more efforts are needed to increase the atomic species to concentrations higher than those at their thermal equilibrium conditions. In the afterglows of mi-

TABLE IV. Probability distribution for product formation in the $^1H+{}^1H_2\rightarrow{}^1H_2+{}^1H$ exchange reaction via a triangular $^1H_3$ transition state.

	Products						
Reactants	$\alpha+\alpha\alpha$	$\alpha+(\alpha\beta+\beta\alpha)$	$\alpha+(\alpha\beta-\beta\alpha)$	$\beta+\alpha\alpha$	$\alpha+\beta\beta$	$\beta+(\alpha\beta+\beta\alpha)$	$\beta+(\alpha\beta-\beta\alpha)$
$\alpha+\alpha\alpha$	1						
$\alpha+(\alpha\beta+\beta\alpha)$		1/3	1/3	1/3			
$\alpha+(\alpha\beta-\beta\alpha)$		1/3	1/3	1/3			
$\alpha+\beta\beta$					1/3	1/3	1/3

crowave discharge, the concentrations of O, S, and halogen atoms were as high as 1–5 % of the total concentrations of their parent molecules [20]. Using selective photodissociation via predissociate states would very likely increase the concentration of atoms. For example, with irradiation by a uv light source at an energy above 175 nm, an O_2 molecule readily dissociates into a metastable $O(^1D)$ atom and a ground state $O(^3P)$ atom via the Schumann-Runge continuum, and the former then relaxes to the ground state.

Over the past decade, much interest has been focused on using lasers to selectively modify chemical species and to create new technological processes at the atomic and molecular level. These modifications and creations could not be achieved using a conventional methodology that operated at thermal equilibrium conditions. The technique described in this work represents a unique approach to these problems with definitive results.

ACKNOWLEDGMENTS

I am indebted to Professor R. A. Bernheim for very useful discussions and encouragement in writing this manuscript. I am grateful for insightful discussions with Drs. D. L. Huestis, P. C. Cosby, and T. G. Slanger. Support from the National Science Foundation is gratefully acknowledged.

APPENDIX

This appendix derives the degree of spin orientation, Θ, and gives its expressions with quantities measured by two commonly used experimental techniques: atomic fluorescence intensity measurement by LIF and laser transmission intensity measurement by absorption spectroscopy. The assumptions used in deriving these expressions are easily satisfied experimentally.

Conventionally, the atom-molecule mixture governed by processes described in Eqs. (1)–(3) is characterized by an equilibrium constant $K_{\rm eq}$,

$$K_{\rm eq}(T)\equiv\frac{k_1}{k_2}=\frac{[{\rm Li}_2]}{[{\rm Li}]^2}. \tag{A1}$$

However, based on the spin multiplicity and bonding versus antibonding nature of molecular potential, Eq. (A1) must be rewritten with the proper electron spin characteristics. For simplicity, first consider an ideal atom (X)–molecule (X_2) system in which the nuclear spin quantum number I equals zero. The equilibrium constant can be written as

$$K'_{\rm eq}(T)=\frac{[X_2]}{[X_{\rm up}][X_{\rm down}]} \quad \text{or} \quad [X_2]=K'_{\rm eq}(T)[X_{\rm up}][X_{\rm down}]. \tag{A2}$$

Without spin orientation, the atom-molecule system has an isotropic spin distribution: the number of atoms with spin ''up'' ($m_s=1/2$) equals the number of atoms with spin ''down'' ($m_s=-1/2$), i.e., $[X_{\rm up}]=[X_{\rm down}]=1/2[X]$. The equilibrium constant $K'_{\rm eq}(T)$ expressed by Eq. (A2) is four times greater than $K_{\rm eq}$ defined by Eq. (A1) for the case of isotropic spin orientation. When the optical pumping laser is turned on, the isotropy of the electron spin distribution is destroyed, with more atoms having spin ''up'' (for the σ^+-polarized laser) or more atoms having spin ''down'' (for the σ^--polarized laser). If we define the degree of spin orientation, ϑ, as

$$\vartheta\equiv\frac{[X_{\rm up}]-[X_{\rm down}]}{[X_{\rm up}]+[X_{\rm down}]}$$

with

$$[X_{\rm up}]+[X_{\rm down}]=[X], \tag{A3}$$

we can reexpress Eq. (A2) in terms of ϑ:

$$\begin{aligned}[X_2]&=K'_{\rm eq}(T,\vartheta=0)\,\frac{[X]}{2}\,(1+\vartheta)\,\frac{[X]}{2}\,(1-\vartheta)\\&=K'_{\rm eq}(T,\vartheta=0)[X_{\rm up}(\vartheta=0)][X_{\rm down}(\vartheta=0)](1-\vartheta^2).\end{aligned} \tag{A4}$$

The molecular density in the atom-molecule system is decreased if ϑ is greater than zero. For complete spin orientation, $\vartheta=1$, $[X_2]=0$. The physical meaning is quite straightforward: without a spin orientation, the collisions between an atom with spin ''up'' and an atom with spin ''down'' are at a maximum value because there are as many atoms with $m_s=1/2$ as there are with $m_S=-1/2$; when ϑ is greater than zero, more atoms are in the $m_s=1/2$ state than in the $m_s=-1/2$ state, or vice versa. The possibility increases for an atom to collide with another atom with the same spin state (triplet state formation). The possibility of forming a stable (singlet state) molecule, therefore, decreases.

The nuclear spin I is often not zero. For alkali-metal atoms, the nuclear spin angular momentum is coupled with electron spin angular momentum, forming hyperfine structures. Under an external magnetic field, the hyperfine levels are further split into hyperfine Zeeman levels, as shown in Fig. 1. Equation (A4) was first derived by Kastler to describe the electron spin orientation on a virtual alkali-metal atom without nuclear spin [13]. However, all alkali-metal atoms and most of the other elements have nonzero nuclear spin angular momenta I, which will couple to electron spins S to form hyperfine structure described by the total spin quantum number F.

Therefore, Eqs. (A3) and (A4) and the definitions of ''$X_{\rm up}$'' and ''$X_{\rm down}$'' do not have valid meaning for atoms with $I\neq 0$. The more general form of the degree of spin orientation takes the form

$$\Theta\equiv\frac{n_a-\langle n^{(k-1)}\rangle}{N} \tag{A5}$$

with

$$\langle n^{(k-1)}\rangle=\frac{\Sigma_{i\neq a}n_i}{k-1} \quad \text{and} \quad N=\sum n_i,$$

where n_a is the number of atoms in the hyperfine Zeeman level into which the atoms are being pumped, n_i is the number of atoms in the ith hyperfine Zeeman level, k is the total number of Zeeman levels involved in the optical pumping transitions, $\langle n^{(k-1)}\rangle$ is the average number of atoms over the $(k-1)$ hyperfine Zeeman levels from which the atoms are

being pumped, and N is the total number of atoms in the ground state manifold. With the definition of the degree of spin orientation Θ by Eq. (A5), Eqs. (A3) and (A4) keep the same form when ''ϑ'' is replaced by ''Θ'' and with the understanding that $X_{\rm up}$ represents atoms having electron spin $m_S=1/2$ (electron spin ''up'') and $X_{\rm down}$ represents atoms having electron spin $m_S=-1/2$ (electron spin ''down''), regardless of their nuclear spin quantum numbers. The quantity Θ defined by Eq. (A5) has a clear physical meaning and is experimentally measurable. It also takes Eq. (A4) as a special case when the nuclear spin $I=0$.

The degree of spin orientation Θ can be determined by measuring atomic fluorescence intensities induced by atomic pumping laser. Under the assumption of low intensity of excitation, N is constant during the optical pumping process, i.e.,

$$\sum_{i\neq a} n_i + n_a = N. \tag{A6}$$

Equation (A5) becomes

$$\Theta = \frac{(k-1)N - k\Sigma_{i\neq a} n_i}{(k-1)N}.$$

Let $\langle n^k(\Theta=0)\rangle$ represent the average population of the k Zeeman levels of the ground state when the optical pumping is off

$$\langle n^k(\Theta=0)\rangle k = N, \tag{A7}$$

Θ then becomes

$$\Theta = \frac{(k-1)\langle n^k(\Theta=0)\rangle - \Sigma_{i\neq a} n_i(\Theta)}{(k-1)\langle n^k(\Theta=0)\rangle}. \tag{A8}$$

If the ground state Zeeman levels are evenly populated when optical pumping is off, i.e.,

$$(k-1)\langle n^k(\Theta=0)\rangle = \sum_{i\neq a} n_i(\Theta=0),$$

we have

$$\Theta = \frac{\Sigma_{i\neq a} n_i(\Theta=0) - \Sigma_{i\neq a} n_i(\Theta)}{\Sigma_{i\neq a} n_i(\Theta=0)}. \tag{A9}$$

Because the fluorescence intensity I_F is proportional to the population in the ground state, the degree of spin orientation Θ can be finally expressed as

$$\Theta = \frac{I_F(\Theta=0) - I_F(\Theta)}{I_F(\Theta=0)}. \tag{A10}$$

The degree of spin orientation Θ can also be determined by measuring transmitted optical pumping laser intensities I_T when optical pumping is turned on and off, respectively. Under the assumption of a weak radiation field, the absorption coefficient α of the sample is constant. The transmitted beam intensity is given by the Lambert-Beer law

$$I_T(\Theta) = I_0 e^{-\langle a(\Theta)\rangle L}, \tag{A11}$$

with L being the absorption path length and $\langle\alpha(\Theta)\rangle$ the average absorption coefficient over L. Because the atomic transition used for optical pumping is usually in the uv or visible region, the population in the excited state is much lower than that of the ground state due to the short lifetime of the upper state. The absorption coefficient α can be expressed in terms of absorption cross section and population in ground state as

$$\alpha = \sigma \sum_{i\neq a} n. \tag{A12}$$

From Eq. (A9), $\Sigma_{i\neq a} n$ can be rewritten as

$$\sum_{i\neq a} n(\Theta) = \left(\sum_{i\neq a} n(\Theta)\right)(1-\Theta) = (k-1)\langle n^{(k-1)}(\Theta=0)\rangle(1-\Theta). \tag{A13}$$

Combining Eqs. (A11)–(A13), we have

$$I_T(\Theta=0) = I_0 \exp[-\langle\sigma\rangle(k-1)\langle n^{(k-1)}(\Theta=0)\rangle L] \tag{A14}$$

when optical pumping is off, and

$$I_T(\Theta) = I_0 \exp[-\langle\sigma\rangle(k-1)\langle n^{(k-1)}(\Theta=0)\rangle(1-\Theta)L] \tag{A15}$$

when optical pumping is on.

Taking logarithms of Eqs. (A14) and (A15), and dividing Eq. (A15) by Eq. (A14), we have

$$\frac{\ln\left[\dfrac{I_T(\Theta)}{I_0}\right]}{\ln\left[\dfrac{I_T(\Theta=0)}{I_0}\right]} = (1-\Theta). \tag{A16}$$

Therefore, Θ can be determined from the signal intensities of transmitted optical pumping laser as

$$\Theta = 1 - \frac{\ln\left[\dfrac{I_T(\Theta)}{I_0}\right]}{\ln\left[\dfrac{I_T(\Theta=0)}{I_0}\right]}. \tag{A17}$$

[1] N. Davidson, *Statistical Mechanics* (McGraw-Hill, New York, 1962), Chap. 9.
[2] H. Middleton *et al.*, Magn. Reson. Med. **33**, 271 (1995).
[3] M. Bloom, in *MTP International Review of Science*, Physical Chemistry Science Series 1, Vol. 4, edited by C. A. McDowell (Butterworths, University Park Press, Baltimore, 1972), p. 1.
[4] J. L. Booth, F. D. Dalby, S. Parmer, and J. Vanderlinde, Chem. Phys. **132**, 209 (1989), and references cited therein.
[5] V. I. Balykin, V. S. Letokhov, V. I. Mishin, and V. A. Semchishen, Chem. Phys. **17**, 111 (1976).

[6] C. He, Ph.D. thesis, The Pennsylvania State University, 1990.
[7] R. A. Bernheim, C. He, and G. Alzetta, J. Chem. Phys. **92**, 5959 (1990).
[8] C. He and R. A. Bernheim, J. Chem. Phys. **95**, 8131 (1991).
[9] W. Happer, Adv. At. Mol. Phys. **24**, 223 (1988), and references cited therein.
[10] A. N. Nesmeyanov, *Vapor Pressure of the Chemical Elements* (Elsevier, Amsterdam, 1963), p. 127.
[11] A. A. Radzig and B. M. Smirnov, *Reference Data on Atoms, Molecules, and Ions* (Springer-Verlag, Berlin, 1985), p. 101.
[12] W. R. Hindmarsh and J. M. Farr, in *Progress in Quantum Electronics*, edited by J. H. Sanders and S. Stenholm (Pergamon Press, Oxford, 1973), Vol. 2, Pt. 4, p. 141.
[13] A. Kastler, Acta Phys. Pol. **34**, 693 (1968).
[14] A. Dalgarno and W. D. Davidson, Adv. At. Mol. Phys. **2**, 1 (1966).
[15] J. C. Whitehead, Mol. Phys. **29**, 177 (1975).
[16] W. H. Gerber and E. Schumacher, J. Chem. Phys. **69**, 1692 (1978).
[17] J. P. Wolf, G. Delacretaz, and L. Woste, Phys. Rev. Lett. **63**, 1946 (1989).
[18] H. G. Weber and M. Stock, Phys. Lett. **50A**, 434 (1974).
[19] With a cell temperature of 463 K and a He-N_2 mixed gas pressure of 30 torr, we achieved $\sim$10% enrichment on ortho-$^{23}Na_2$ over para-$^{23}Na_2$. ^{23}Na atoms were spin aligned by a multimode R6G dye laser with 50 mW output power at 589 nm, and the concentrations of ortho-$^{23}Na_2$ and para-$^{23}Na_2$ dimers were monitored by an Ar^+ laser operated at 488 and 496.5 nm, respectively.
[20] M. F. Golde and B. A. Thrush, Rep. Prog. Phys. **36**, 1285 (1973).